Journal of Applied Electrochemistry **30**: 891–897, 2000.

Reduction of hexavalent chromium by copper

S. GOERINGER, N.R. de TACCONI, C.R. CHENTHAMARAKSHAN and K. RAJESHWAR*
*Department of Chemistry and Biochemistry, The University of Texas at Arlington, Arlington, TX 76019-0065, USA (*author for correspondence, fax: (817)-272-3808, e-mail: rajeshwar@uta.edu)*

Received 27 August 1999; accepted in revised form 29 February 2000

Key words: environmental remediation, first-order kinetics, mass transport, medium pH

Abstract

The galvanic reaction of metallic copper in Cr(VI)-laden aqueous solutions of varying pH was examined by *in situ* u.v.–visible spectrophotometry, rotating disc electrode chronopotentiometry and cyclic voltammetry. The galvanic reaction in 0.2 M H_2SO_4 solutions was pseudo first order in Cr(VI) concentration. Experiments with both magnetically stirred solutions and a copper mesh or a copper film in a rotating disc electrode configuration revealed the reaction to be diffusion-controlled with respect to Cr(VI) transport to the copper surface. Finally, cyclic voltammetry data in Cr(VI)-laden media of varying pH underline the important role of protons in the galvanic reaction.

1. Introduction

Chromium exists in two common oxidation states in nature, Cr(III) and Cr(VI). Hexavalent chromium is toxic and carcinogenic while the element in its trivalent state is an essential nutrient for plant and animal metabolism in trace amounts. Hexavalent chromium is also notoriously mobile in nature because it is only weakly bound to inorganic surfaces. However, Cr(III) behaves like Fe(III) in the environment, being readily precipitated at near neutral pH. Thus reduction of chromium to the trivalent state usually serves to immobilize it.

On the one hand, depending on the medium pH, hexavalent chromium is thermodynamically stable in the presence of O_2 and its reduction in aerobic environments is an endoergic process. On the other hand, the short-term stability of dichromate solutions in water has a kinetic origin since water is thermodynamically capable of reducing Cr(VI). It is of interest to explore how common metals such as copper behave toward Cr(VI) aqueous solutions. We have recently shown [1–4] that carbonaceous materials such as carbon black and organic polymers such as polypyrrole can reduce Cr(VI). In these cases as with copper, the galvanic reaction occurs at the solid material/solution boundary. The reduction reaction:

$$\begin{aligned} &Cr_2O_7^{2-} + 14\,H^+ + 6\,e^- \leftrightarrow 2\,Cr^{3+} + 7\,H_2O \\ &E^\circ = 1.33\,V \text{ vs SHE} \end{aligned} \quad (1)$$

requires an abundant supply of protons as well as efficient mass transport of Cr(VI) to the reductant surface since this is a heterogeneous reaction.

In this study we combine a number of experimental techniques including *in situ* u.v.–vis. spectrophotometry, cyclic voltammetry, and chronopotentiometry in a rotating disc electrode (RDE) configuration to study the reaction of Cr(VI) with copper. We show below that medium pH and Cr(VI) mass transport are crucial factors in controlling the rate of reduction of Cr(VI) and the dissolution of copper. An early study using RDE voltammetry [5] is of particular relevance to the present one as elaborated below.

Aside from fundamental considerations, there is also a practical incentive for studying the title reaction. The toxicity of chromium has prompted a severe curtailment in its technological use and the search for environmentally more benign substitutes. In spite of this, however, new strategies for remediation of water streams bearing this element continue to be important, either because complete replacement of Cr(VI) is not feasible or because of problems with leaching from old dumpsites to aquifers.

Both hexavalent chromium and copper are ubiquitous in the microelectronics industry. Thus an examination of the reactivity of copper surfaces in Cr(VI) solutions would also have relevance from a materials processing perspective.

2. Experimental details

2.1. *Chemicals*

Potassium dichromate from Baker and cupric sulfate from Spectrum were both ACS Reagent Grade and were used without further purification. The copper mesh (50 mesh from 0.23 mm diameter wire) was from Alfa

Aesar. Deionized, distilled water was used for preparing all solutions.

2.2. *Instrumentation*

The u.v.–vis. spectrophotometry experiments were run on a Hewlett Packard 8425 diode array spectrometer. Potential/current control and cyclic voltammetry experiments both utilized an EG&G Princeton Applied Research (model 273) potentiostat/galvanostat. The rotating disc electrode (RDE) was manufactured by Pine Instrument Co. and the set-up included an AFMSR rotor connected to a RDE4 potentiostat.

2.3. *Procedures*

The reaction of Cr(VI) with the copper mesh was monitored *in situ* using u.v.–vis. spectrophotometry. Modifications to a 1 cm quartz cuvette top facilitated the placement of both the copper mesh as well as a Pt wire and a Ag/AgCl/3 M KCl microreference electrode so that the effect of applying a potential (or current) to the copper mesh (via a potentiostat three-electrode arrangement) could be probed. The Cr(VI) solution in the cuvette could also be magnetically stirred. The alternative thin-layer cell assembly usually employed for spectroelectrochemical experiments [6, 7] was initially considered but not utilized for this study because the present design better facilitated solution exchange and cleaning of the copper mesh between runs.

For the RDE chronopotentiometry experiments, a Pt disc (Pine Instrument Co.) plated with a copper film was used. The disc was washed with 50% HNO_3 and polished with 0.03 μm alumina (Buehler). The plating bath consisted of 0.2 M $CuSO_4$ in 0.1 M H_2SO_4. The disc was rotated at 52.4 rad s^{-1} (unless otherwise noted) and a plating current of 1 mA was applied for varying time. The change in potential of the copper-plated Pt RDE on contact with Cr(VI)-laden 0.2 M H_2SO_4 solutions was monitored on an Omnigraphic 2000 (Houston Instruments) time-base recorder.

All Cr(VI) solutions and the copper plating baths were purged with prepurified N_2 for several minutes (normally ~15 min) prior to an experiment. The copper mesh (geometric area: 1.35 cm^2 unless otherwise noted) was used as received for all the experiments. Preliminary experiments using an acid wash (to remove the native oxide skin of the mesh) yielded irreproducible results presumably because of varying degrees of oxide film removal.

Cyclic voltammetry also utilized the Cu mesh as working electrode with a Pt wire as the counter electrode and Ag/AgCl/3 M KCl as the reference in these experiments. The potential sweep rate was 20 mV s^{-1}.

All measurements below pertain to the laboratory ambient temperature.

3. Results and discussion

3.1. *Spectrophotometric data on the reduction of Cr(VI) by copper*

Figure 1 contains a series of u.v.–vis. spectra obtained *in situ* (see Section 2) when a 1 mM $K_2Cr_2O_7$/0.2 M

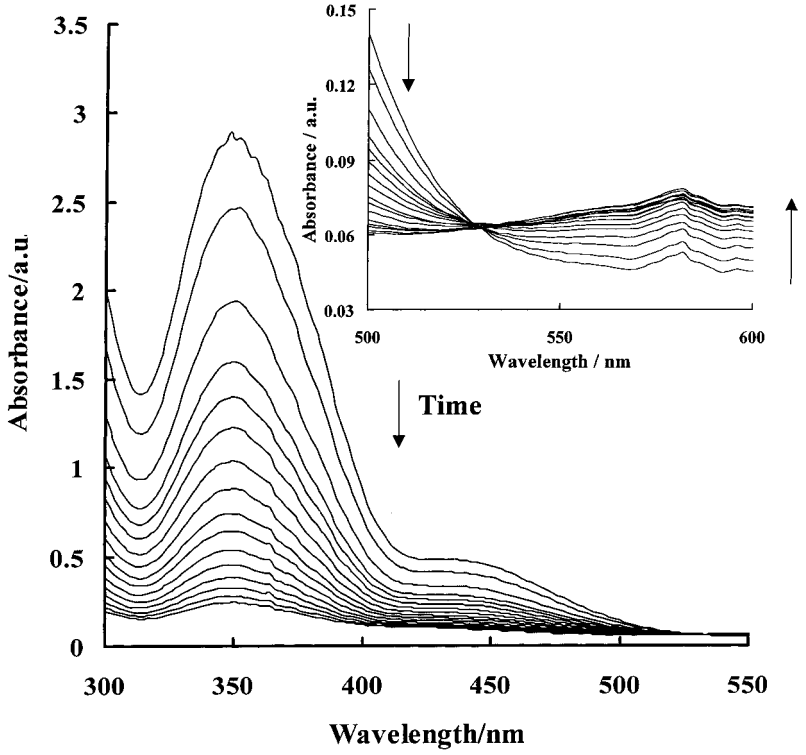

Fig. 1. In situ u.v.–vis. spectral profiles as a copper mesh undergoes dissolution in a 1 mM $K_2Cr_2O_7$/0.2 M H_2SO_4 medium. Inset amplifies changes in the 500–600 nm wavelength range.

H_2SO_4 solution was contacted with the copper mesh. The spectra were acquired every 4 min for 1 h in Figure 1; the peak at ~350 nm is due to absorption by the Cr(VI) species [1–3]. The absorbance is seen to steadily decay as the Cr(VI) is reduced by copper. Concomitantly, the spectral feature due to the Cu^{2+} species generated evolves at longer wavelengths in the 570–590 nm range as shown in the insert in Figure 1. There is also an isosbestic point at ~530 nm.

Data such as these in Figure 1 were acquired for varying Cr(VI) concentrations in the 0.2–1.0 mM range. Figure 2(a) contains the temporal profiles of the absorbance at 350 nm. Further analyses of these data according to Figure 2(b) show that they are reasonably well described by first-order kinetics with respect to Cr(VI). Least-squares analyses of the plots in Figure 2(b) yield a first-order rate constant of 4.4×10^{-2} min^{-1} with a nominal uncertainty of ±15%.

Recalling that protons are also co-reactants in the Cr(VI) reduction reaction, (Equation 1), kinetics experiments as in Figure 2 were repeated for a range of proton concentrations from 0.02 to 0.2 M. Within the error limits quoted above, no variations in the reduction rate were noted. Thus we have a pseudo-first order kinetics situation in this study since the protons are in large excess relative to Cr(VI) in these experiments.

The effect of Cu mesh area on the Cr(VI) reduction rate was also probed; the results are contained in Figure 3. Given the heterogenous nature of the reaction, the extracted rate constants can be 'normalized' by the geometric factor, A/V (A: copper surface area, V:

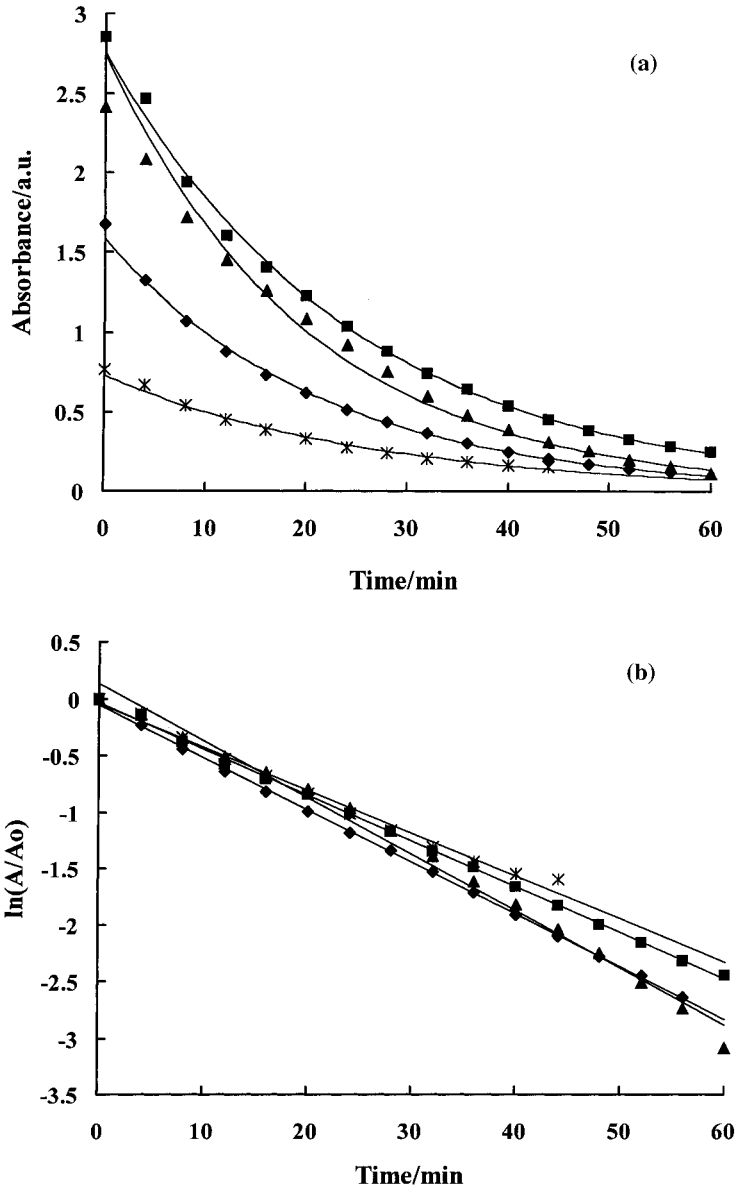

Fig. 2. (a) Temporal profiles of the 350 nm absorbance for *x* mM $K_2Cr_2O_7$/0.2 M H_2SO_4 solutions. Data acquired as in Figure 1. *x* in mM: (∗) 0.2, (◆) 0.5, (▲) 0.8 and (■) 1.0. (b) First-order rate law plots of the data in Figure 2(a). Lines in Figure 2(a) and (b) are least-squares fits of the data points.

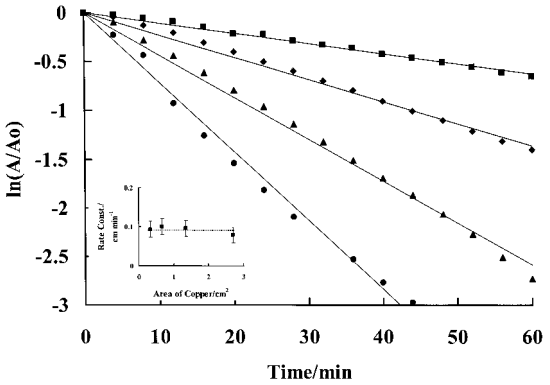

Fig. 3. As in Figure 2(b), but with varying geometric area (A) for the copper mesh. A in cm^2 from top to bottom: 0.34, 0.68, 1.35 and 2.7. The lines are least-squares fits of the data points. Insert shows normalized rate constants (see text) extracted from these plots as a function of the copper mesh surface area.

solution volume) [5]. When this is done, the reduction rate is seen to be independent of the copper surface as depicted in the insert in Figure 3. As mentioned in the Experimental section, the experiments were done with a nominal surface area of the mesh of 1.35 cm^2.

Figure 4 compares the temporal profile in Cr(VI) absorbance at open-circuit (–0.03 V vs Ag/AgCl) in the Cu–Cr(VI) system with two other cases where a bias potential was applied to the copper mesh. These data pertain to a 1 mM $K_2Cr_2O_7$/0.2 M H_2SO_4 solution. On the one hand, the galvanic system can be perturbed in either direction by the electrical bias; a positive potential applied to the copper mesh (relative to its rest point) accelerates its dissolution. On the other hand, when the copper anode is poised at a potential negative of its rest value, the galvanic reaction is impeded. This latter situation is rather akin to that existing in a cathodic protection strategy for a surface against corrosion.

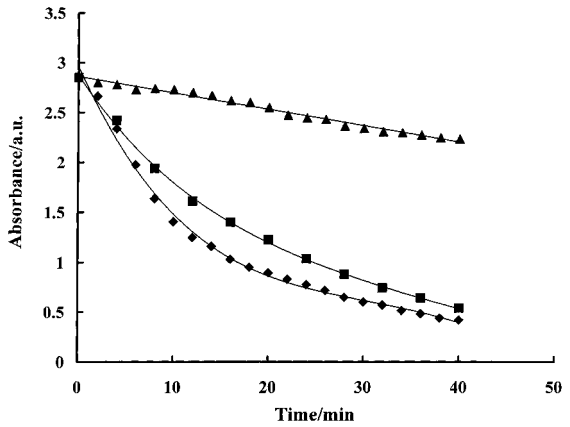

Fig. 4. Temporal profiles of the 350 nm absorbance for a reaction medium as in Figure 1. Three scenarios are compared corresponding to: (■) open-circuit, (◆) 0.15 V and (▲) −0.10 V (all potentials with respect to Ag/AgCl reference) for the copper mesh in the medium. Lines are least-squares fit of data points.

3.2. *Mass transport considerations*

As mentioned earlier in an introductory paragraph, mass transport of Cr(VI) to the copper surface plays an important role given that the reaction is heterogeneous. The data in Figures 2–4 pertain to the unstirred condition of the Cr(VI)-laden solution. Stirring and convective transport clearly aid the reaction kinetics as shown by the data in Figure 5. In all the cases, however, the reaction remains pseudo first-order with respect to Cr(VI) (Figure 5(b)) with the rate constants in min^{-1} increased from the unstirred condition (see above) to 8.3×10^{-2}, 14.1×10^{-2}, and 19.1×10^{-2} at low, medium, and high stir speeds respectively for a Cu mesh of 1.35 cm^2.

More precisely defined hydrodynamic conditions may be imposed by electrode rotation, rather than by magnetic stirring [8]. Indeed previous authors [5] have used a copper RDE to study its dissolution in sulfuric acid solutions with the dichromate ion added as a

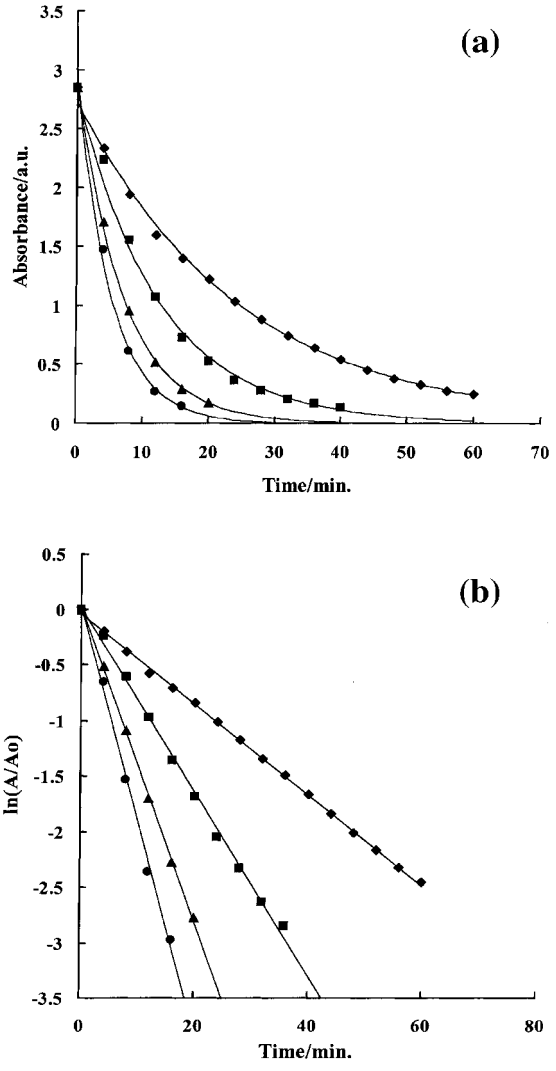

Fig. 5. As in Figure 2 but for varying stir rates of a 1 mM $K_2Cr_2O_7$/0.2 M H_2SO_4 solution: (◆) no stirring, (■) low speed, (▲) medium speed and (●) high speed.

depolarizer. By studying the effect of temperature and rotation speed at high and low acid concentrations, the dissolution process was shown to be determined completely by the rate of transport of the depolarizer to the reacting surface [5].

The importance of Cr(VI) mass transport in its reaction with copper was also explored in the present study using a RDE configuration for the copper surface. However, instead of RDE voltammetry (cf. [5]), we decided to adopt a chronopotentiometry approach to heterogeneous reaction kinetics as described by recent authors [9]. In essence the time taken to dissolve a copper film on the RDE surface was measured in this approach as a function of three variables: namely, the plating time, the rotation speed and the Cr(VI) concentration.

The dissolution time (t_d) is determined potentiometrically (see Figure 6) as the time between the start of the reaction (i.e., when the copper film is immersed in the Cr(VI) medium) and the point where the copper potential rises sharply [9]. The average reaction rate, R (mol m^{-2} s^{-1}) is then given by:

$$R = N/At_d \tag{2}$$

where A is the copper geometric area (taken to be equal to the reaction area under the diffusion-limited conditions, [9, 10]). In Equation 2, N is the number of moles of copper plated out. Thus,

$$N = \eta I_p t_p/2F \tag{3}$$

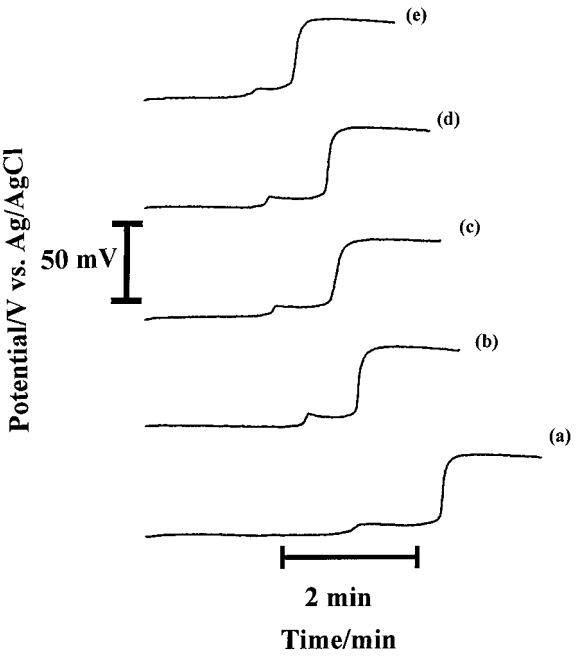

Fig. 6. Chronopotentiograms for the dissolution of a copper film in 1 mM $K_2Cr_2O_7$/0.2 M H_2SO_4 as a function of electrode rotation speed (in rad s^{-1}): (a) 52.4, (b) 104.7, (c) 157.1, (d) 209.4 and (e) 261.8. Plating current was 1 mA, plating time was 30 s and geometric area of the RDE was 0.196 cm^2. See also Figure 7(b) below.

In Equation 3, η is the current efficiency, I_p is the plating current (nominally 1 mA here) and t_p is the plating time. Combining Equations 2 and 3,

$$t_p = (2AFR/\eta I_p)t_d \tag{4}$$

Thus a plot of t_p against t_d, for a constant set of reaction conditions, should be a straight line through the origin. Figure 7(a) illustrates this for the present Cr(VI)-copper reaction case. The slope of this plot (m) is characteristic of the rate of dissolution under a given set of experimental conditions (see Equation 4) [9]. An m value of ~1.07 was obtained by previous authors [9] for the reaction:

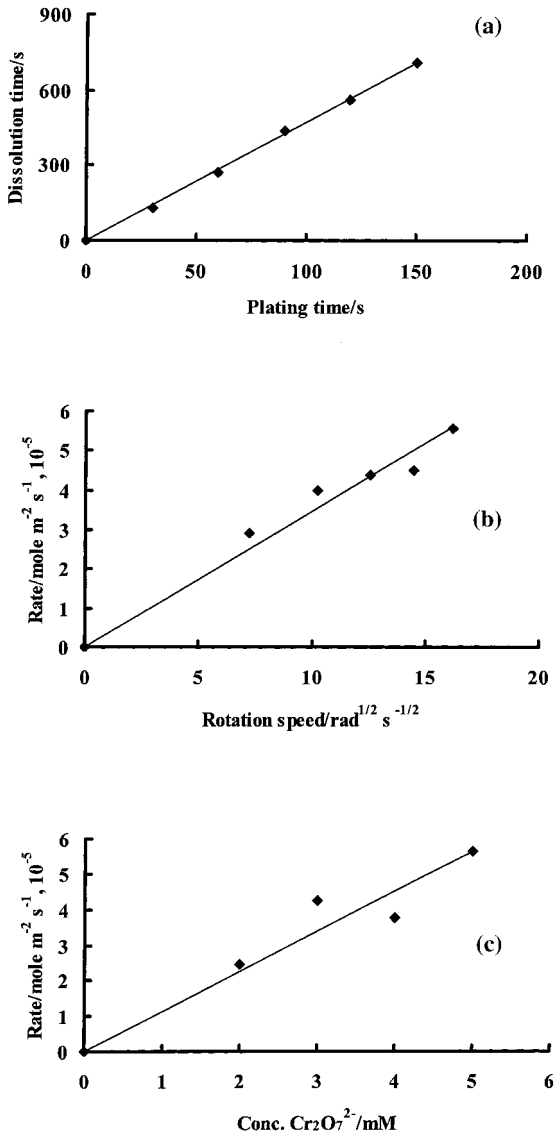

Fig. 7. (a) Plot of the dissolution time versus plating time (Equation 4) for a Cu film RDE (angular rotation speed 52.4 rad s^{-1}) in 1 mM $K_2Cr_2O_7$/0.2 M H_2SO_4. Other conditions as in Figure 6. (b) Effect of RDE rotation speed on the reaction rate as defined by Equations 2 and 7. Other conditions as in Figure 6. (c) Effect of Cr(VI) concentration on the reaction rate (Equation 7) with the angular rotation speed at 52.4 rad s^{-1} and other conditions as in Figure 6. Lines in all cases are least-squares fits of data points.

$$Cu + Fe^{3+} \rightarrow Cu^{+} + Fe^{2+} \quad (5)$$

However, an m value of ~ 5 is obtained in the present case consistent with the fact that Cr(VI) is a 6-electron oxidant while Fe(III) is a 1-electron oxidant. It is also pertinent to note that unlike in the study in [9], a noncomplexing medium that does *not* stabilize Cu^{+} was used here. Also, the current efficiency term in Equation 4 can be ignored since it is close to unity for the particular plating process considered here [9].

If the reaction is mass transport controlled (Figure 5), the flux (J) of Cr(VI) to the copper surface should be equal to the rate of copper dissolution:

$$J = R \quad (6)$$

For a RDE configuration, J is well-described by the Levich equation [8].

$$J = 0.62 D^{2/3} v^{-1/6} \omega^{1/2} C \quad (7)$$

In Equation 7, D is the diffusion coefficient of Cr(VI), v is the kinematic viscosity of the medium, ω is the angular rotation speed and C is the bulk Cr(VI) concentration.

According to Equation 7, a plot of the reaction rate vs. either $\omega^{1/2}$ or C should be linear passing through the origin. The data in Figure 7(b) and (c) are in accord with this expectation. Using a value of 1.004×10^{-6} m^2 s^{-1} for v [11], the slopes (determined by least-squares fits of the data points) in Figures 7(b) and (c) correspond to 0.347×10^{-5} mol m^{-2} s$^{-1/2}$ and 1.131×10^{-5} m s^{-1}, respectively. These, in turn, yield values for D of 4.2×10^{-10} m^2 s^{-1} and 5.0×10^{-10} m^2 s^{-1}, respectively, for dichromate ions in 0.2 M H_2SO_4. We are not aware of values in the literature for comparison. However, the present data fall well within the range of values characteristic of multivalent ions in aqueous media [8, 9, 11].

One final point with regard to the data presented in the section concerns the potential–time profiles (e.g., see Figure 6). An initial hump was present in all the cases in the potential, followed by a plateau. This was then followed by an abrupt larger jump in the copper potential (Figure 6). We attribute the initial (weaker) feature to dissolution of the native oxide skin on the copper surface. The dominant potentiometric feature then corresponds to oxidation of the bulk metal. This is further elaborated by cyclic voltammetry as discussed next.

3.3. *Cyclic voltammetry*

As described in the Experimental section, the copper mesh was used as the working electrode in contact with 1 mM $K_2Cr_2O_7$ solutions in either 0.2 M KNO_3 or 0.2 M H_2SO_4. In each case, the potential was initially swept in the negative direction from the rest condition (about −0.03 V vs Ag/AgCl). Figure 8 contains two sets of cyclic voltammetry (CV) data illustrating the influence of Cr(VI) on copper electrochemistry in a neutral pH (0.2 M KNO_3) medium. An initial cathodic wave in Figure 8(a) between −0.7 V and −0.8 V (all potentials hereafter are quoted with respect to the Ag/AgCl reference) corresponds to reduction of the native oxide skin on the copper surface (see above) as assessed by separate measurements in this laboratory. On the return cycle an anodic loop distinctive of copper dissolution is seen close to the positive potential limit. On the second, negative-going scan, the copper ions generated by dissolution are redeposited culminating in the wave at about −0.2 V. Native copper oxides are concomitantly formed and these are reduced in the second cathodic wave prior to the solvent breakdown limit.

Dramatic changes in the CV profiles occur when Cr(VI) is added to the 0.2 M KNO_3 medium (Figure 8(b)). Both the solvent breakdown current flow and the copper dissolution loop are greatly attenuated near the two

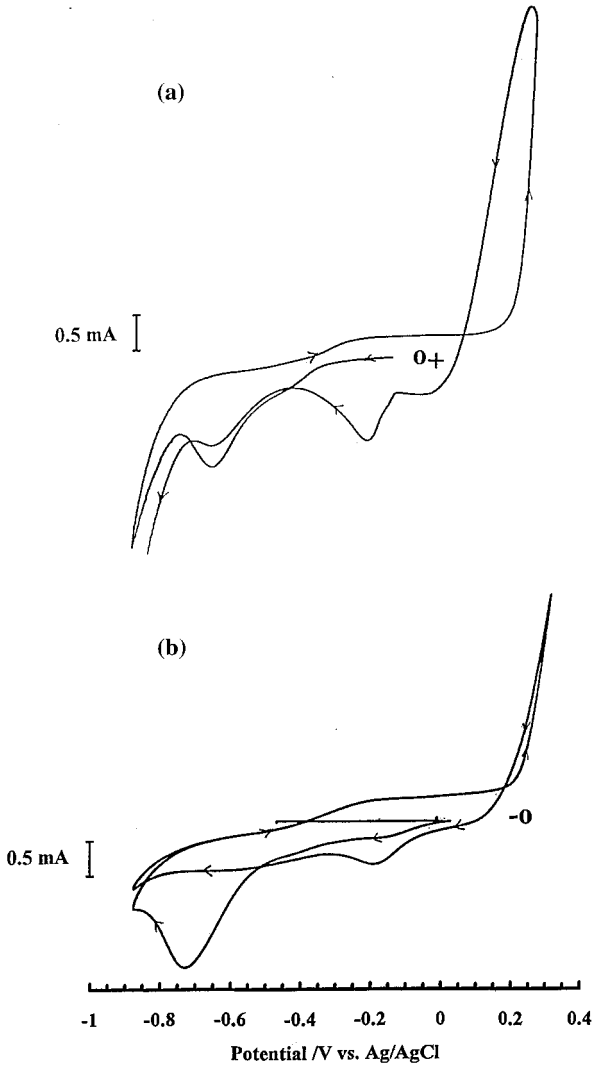

Fig. 8. Cyclic voltammograms from −0.85 to 0.40 V for a copper mesh in (a) 0.2 M KNO_3 and (b) 0.2 M KNO_3 + 1 mM $K_2Cr_2O_7$. In each case, initial scan began from rest (see text) in the negative direction. Two cycles are shown.

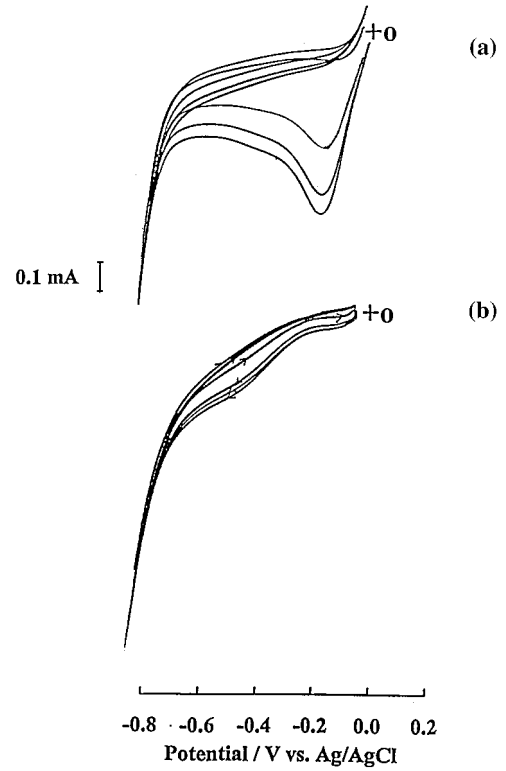

Fig. 9. Cyclic voltammograms for a copper mesh in: (a) 1 mM $K_2Cr_2O_7$/0.2 M H_2SO_4 solution with increasing time delays between cycles of 1, 2 and 3 min, respectively. Initial scan began from rest potential in negative direction. (b) As in Figure 9(a) but for 0.2 M H_2SO_4 'control' medium instead.

limits of the scans. Passivation of the electrode surface by adsorption of the dichromate ions can explain the two trends seen in Figure 8(b). The galvanic oxidation of copper by Cr(VI) is negligible (because of inadequate proton supply) although it is thermodynamically feasible. Thus the Cu^{2+} ion redeposition peak and the copper oxide reduction wave are both attenuated (relative to Figure 8(a)) on the second, negative-going scan.

When the pH is lowered and the ratio of proton concentration to Cr(VI) concentration is high (as in experiments considered in the earlier sections), the galvanic reaction sets in and drastically alters the CV profile (Figure 9(a)). The copper dissolution loop (see Figure 8(a)) was conspicuous by its absence (data not shown in Figure 9). The copper redeposition wave increases in amplitude with each scan as the galvanic reaction (generating Cu^{2+}, Figure 1) progresses. In Figure 9(a), three negative-going scans are shown corresponding to increasing time delays of 1, 2 and 3 min at the positive potential limit. The copper re-deposition wave grows in amplitude albeit in a non-linear manner. In fact, this wave grows in amplitude as $t^{1/2}$ diagnostic of the diffusion of copper ions away from the working electrode vicinity. Figure 9(b) contains control CV scans (performed identically as in Figure 9(a)) but in 0.2 M H_2SO_4 in the absence of Cr(VI). Clearly, the Cu^{2+} reduction features (that are induced by Cr(VI)) are absent here.

4. Conclusions

This study demonstrates that with only simple modifications, u.v.–vis. spectrophotometry can be profitably employed for *in situ* monitoring of galvanic reactions such as the oxidation of copper by Cr(VI). The galvanic reaction is found to be pseudo-first order (with respect to Cr(VI)) for proton concentrations in the medium ranging from 0.02 to 0.2 M. Chronopotentiometry (performed in a RDE mode) and cyclic voltammetry afford further mechanistic insights into the galvanic reaction.

References

1. C. Wei, S. German, S. Basak and K. Rajeshwar, *J. Electrochem. Soc.* **140** (1993) L60.
2. W.A. Wampler, S. Basak and K. Rajeshwar, *Carbon* **34** (1996) 747.
3. R. Senthurchelvan, Y. Wang, S. Basak, and K. Rajeshwar, *J. Electrochem. Soc.* **143** (1996) 44.
4. Y. Wang and K. Rajeshwar, *J. Electroanal. Chem.* **425** (1997) 183.
5. D.P. Gregory and A.C. Riddiford, *J. Electrochem. Soc.* **107** (1960) 950.
6. G-W. Jang, E.W. Tsai and K. Rajeshwar, *J. Electrochem. Soc.* **134** (1987) 2377.
7. G-W. Jang, E.W. Tsai and K. Rajeshwar, *J. Electroanal. Chem.* **263** (1989) 383.
8. R.N. Adams, 'Electrochemistry at Solid Electrodes' (Marcel Dekker, New York, 1969), chapter 4.
9. K.J. Drok, I.M. Ritchie and G.P. Power, *J. Chem. Ed.* **75** (1998) 1145.
10. F. Opekar and P. Beran, *J. Electroanal. Chem.* **69** (1976) 1.
11. 'Handbook of Chemistry and Physics', 60th edn (CRC Press, Boca Raton, FL, 1979).